Spectroscopy of the ^{10}Li nucleus

J. A. Caggiano,* D. Bazin, W. Benenson, B. Davids, B. M. Sherrill, M. Steiner, J. Yurkon, and A. F. Zeller
National Superconducting Cyclotron Laboratory, Michigan State University, East Lansing, Michigan 48824

B. Blank
Centre d'Etudes Nucléaires de Bordeaux-Gradignan, F-33175 Gradignan Cedex, France

(Received 28 June 1999; published 22 November 1999)

In an attempt to clarify the situation regarding the low-lying structure of ^{10}Li, a spectroscopic measurement of the structure of ^{10}Li with the ^{9}Be(^{9}Be,^{8}B)^{10}Li reaction at $E(^{9}\mathrm{Be})=40.1(1)$ MeV/nucleon was performed using the S800 spectrograph at Michigan State University. The data are fit best with a single *p*-wave resonance at $-S_n=0.500(60)$ MeV with a width of $\Gamma=400(60)$ keV. No higher lying states were observed and there is no evidence of a state at $\sim$250 keV in the data. An excess strength at threshold was observed, but cannot be definitively attributed to a state. [S0556-2813(99)05211-5]

PACS number(s): 21.10.−k, 25.70.Hi, 27.20.+n

I. INTRODUCTION

It is a well known effect of quantum mechanics that the wave function of a particle in a well can significantly penetrate the potential barrier if the separation energy is low. This effect is observed in nuclei in which the last few valence nucleons are weakly bound. In some cases, such as ^{11}Li, the probability of finding a valence neutron outside the core nucleus is more than 90% [1]. Put another way, the valence rms radius for ^{11}Li is 9.5 fm while the ^{9}Li core rms radius is only 2.3 fm [2]. In this case the extent of the penetrating wave function is much larger than the range of the nuclear force. This type of nucleus is called a halo nucleus and represents a new form of nuclear matter, characterized by a central normal nucleus and a halo of penetrating wave function. It is interesting to investigate how well standard nuclear models, such as the shell model, can describe the properties of these nuclei. Certain cases such as ^{11}Li are particularly interesting because here the last two neutrons are weakly bound. Hence the halo has two neutrons, and the interactions of these neutrons in the diffuse nuclear surface largely determine the properties of ^{11}Li [3].

The nucleus ^{10}Li has been the subject of much experimental study, primarily due to its importance for the study of ^{11}Li. It has been speculated that the best model for ^{11}Li is a three-body system. Many authors have accurately calculated ^{11}Li properties with three-body models [4–6]. However, these attempts to understand ^{11}Li rely on the nature of the interaction between the two-body subsystems, *n*-*n* and *n*-^{9}Li. The *n*-*n* interaction is well known, but the *n*-^{9}Li interaction is not well understood. Information about the *n*-^{9}Li interaction is best obtained through experimental study of the unbound nucleus ^{10}Li. All attempts to compare three-body and standard models of ^{11}Li rely on the ^{10}Li data, yet the existing experimental situation is unclear.

It is most likely that the ground state of ^{10}Li is either a $0p_{1/2}$ or an $1s_{1/2}$ neutron coupled to the $0p_{3/2}$ proton, giving rise to states with J^{π} assignments of $(1^{+},2^{+})$ or $(1^{-},2^{-})$, respectively. Theoretical arguments have been made to show that the ground state of ^{10}Li might be an *s*-wave state. Barker and Hickey predicted in 1977 that the ^{10}Li ground state is a virtual *s* state [7], as is the case with its isotone ^{11}Be. Some shell-model calculations [8,9] suggest that the *s*-wave (2^{-}) state is the ground state, while other calculations [10,11] suggest that a *p*-wave state (1^{+}) may be the ground state.

There is no consensus on ^{10}Li structure based on experimental work [11–18] (see Table I) and the difficulty of studying this nucleus is well documented. Wilcox *et al.* [12] saw roughly 30 counts with poor resolution in a peak identified as the ^{10}Li ground state unbound by 800 keV. Amelin *et al.* [13] observed a broad peak unbound by 150 keV which was identified as the ^{10}Li ground state. Young *et al.* [14] had roughly twice the number of events, and saw some evidence for a low-lying, possibly *s*-wave state at <100 keV in addition to a higher-lying *p*-wave state at 540 keV. Bohlen *et al.* [15] have seen several structures, in particular resonances at 240 and 530 keV, attributed to *p*-wave resonances. Kryger *et al.* [16] and Thoennessen *et al.* [17] saw a narrow peak in a ^{9}Li-*n* relative velocity spectrum from the fragmentation of ^{18}O, which may be interpreted as a low-lying s-wave state at 50 keV or a higher lying state decaying to a ^{9}Li excited state. Unfortunately, most spectroscopic measurements of ^{10}Li structure to date have been hindered by poor statistics, poor resolution, target contaminants, or some combination of all three. The fact that the states are unbound, broad, and asymmetric have also made experimental study difficult.

Unfortunately, no definitive measurement of ^{10}Li has been made. With this in mind, we set out to measure the low-lying resonance structure of ^{10}Li using the newly commissioned S800 spectrograph at Michigan State University [19]. The goal of the experiment was to make a clean, high-resolution, high-statistics spectroscopic measurement of ^{10}Li near threshold.

II. EXPERIMENT

The spectrograph is designed to have an energy resolution of $E/\Delta E=10\,000$, an angular resolution of $\leqslant 2$ mrad, and a

*Present address: Argonne National Laboratory, 9700 S. Cass Ave., Argonne, IL 60439.

TABLE I. Previous measurements of ^{10}Li low-lying resonances. The energies, widths, and uncertainties of the observed resonances below $-S_n=1$ MeV are listed as well as the year that the data were published, and any assignment given by the authors.

Author	Year	Reaction	$-S_n$ (MeV)	Γ (MeV)	Assignment
Wilcox *et al.* [12]	1975	^{9}Be(^{9}Be,^{8}B)^{10}Li	0.80(25)	1.2(3)	g.s.
Amelin *et al.* [13]	1990	^{11}B(π^-,p)^{10}Li	0.15(15)	<0.4	$s_{1/2}$ g.s.
Kryger *et al.* [16]	1993	^{18}O fragmentation	<0.15		g.s.
			or ≈ 2.5		excited state
Young *et al.* [14]	1994	^{11}B(^{7}Li,^{8}B)^{10}Li	0.54(6)	0.36(2)	$p_{1/2}$
			<0.10	<0.23	$s_{1/2}$ g.s.
Bohlen *et al.* [15]	1997	^{9}Be(^{13}C,^{12}N)^{10}Li	0.53(6)	0.30(8)	
		^{10}Be(^{12}C,^{12}N)^{10}Li	0.24(6)		$p_{1/2}$
Zinser *et al.* [18]	1997	^{11}Li breakup	0.21(5)	0.12(+0.10,−0.05)	
			0.62(10)	0.6(1)	
Bertsch *et al.* [6]	1998	^{11}Li breakup [a]	0.05(2)		$s_{1/2}$ g.s.
			0.25(4)		$p_{1/2}$
Thoennessen *et al.* [17]	1999	^{18}O fragmentation	<0.05		g.s.

[a]This is a reanalysis of Zinser data [18].

20 msr acceptance. It consists of a beam analysis line and the spectrograph itself. The beam analysis line is very similar to the A1200 fragment separator at MSU [20], but with larger acceptance and better resolution. The spectrograph consists of a large, superconducting quadrupole doublet followed by two 70-ton superconducting dipole magnets. The detectors in the focal plane consist of two position tracking detectors separated by approximately one meter, an ion chamber for energy-loss measurements, and three thick plastic scintillators for total energy measurement [21] (see Fig. 1).

The spectrograph was operated in dispersion-matched mode to cancel the 0.08(1)% intrinsic beam energy spread. Ray-tracing techniques were used to reconstruct the energy of the ejectile from the target. The measured magnetic-field data were used as input to a particle optics code COSY [22]. COSY calculates a transfer map from the target to the focal plane under the assumption that the incoherent beam spot is small, and the dispersion matching is perfect. The transfer map is then inverted, and with measurement of horizontal and vertical positions and angles in the focal plane, it is possible to deduce the energies, angles, and vertical positions of the emerging nuclei from the reaction in the target using the procedure described in Berz *et al.* [23].

The S800 was used to make a spectroscopic measurement of the ^{9}Be(^{9}Be,^{8}B)^{10}Li reaction in order to study states in

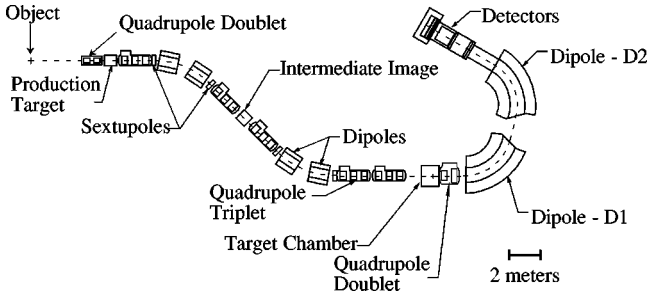

FIG. 1. The S800 spectrograph.

^{10}Li. This reaction was chosen because it is reported to have a reasonably large cross section [12]. Also, the ^{8}B ejectile has a much different rigidity than other competing reactions, which leads to a relatively contaminant-free focal plane. A beam of 40.1(1) MeV/nucleon ^{9}Be was used to bombard three targets: 0.94(9) mg/cm^2 Be, 1.1(1) mg/cm^2 carbon, and a 0.45(3) mg/cm^2 Be target on a formvar backing. The ^{8}B and ^{11}C reaction products were transported to the focal plane of the spectrograph, where the two transverse positions, angles, and total energies of the ions were measured. The reaction scattering angles and energies were reconstructed with ray-reconstruction techniques [23] as described above. The ^{12}C(^{9}Be,^{8}B)^{13}B and ^{12}C(^{9}Be,^{11}C)^{10}Be reactions were used for energy calibration (the ground-state Q values are -28.1356 MeV and -11.9091, respectively [24]). These reactions populated several known states in ^{13}B and two states in ^{10}Be.

Elastic and inelastic scattering of the incident ^{9}Be beam off the targets provided calibration of the spectrograph bending radius and scattering angle. The relationship between the relative bending radius of the spectrograph and the focal plane position was calibrated by sweeping the elastically scattered peak across the focal plane by varying the magnetic field. The known central bend radius of the S800 and the two different energy calibration reactions were used to determine the beam energy of 40.1(1) MeV/nucleon.

The small amount of hydrogen and oxygen contaminants in the carbon target as well as the formvar backing (carbon, hydrogen, and oxygen) on the thin beryllium target provide excellent scattering angle calibration ($\pm 0.05°$). Figure 2 shows a kinematic energy spectrum of reconstructed scattering angle versus energy for elastic and inelastic scattering off the carbon target with hydrogen and oxygen (probably water) contamination. Elastic lines from the three nuclei are clearly visible as are inelastic scattering to the 4.44(2^+), 7.65(0^+), and 9.64(3^-) MeV states of ^{12}C and the natural parity doublets at 6.09 and 7.02 MeV in ^{16}O. All lines drawn

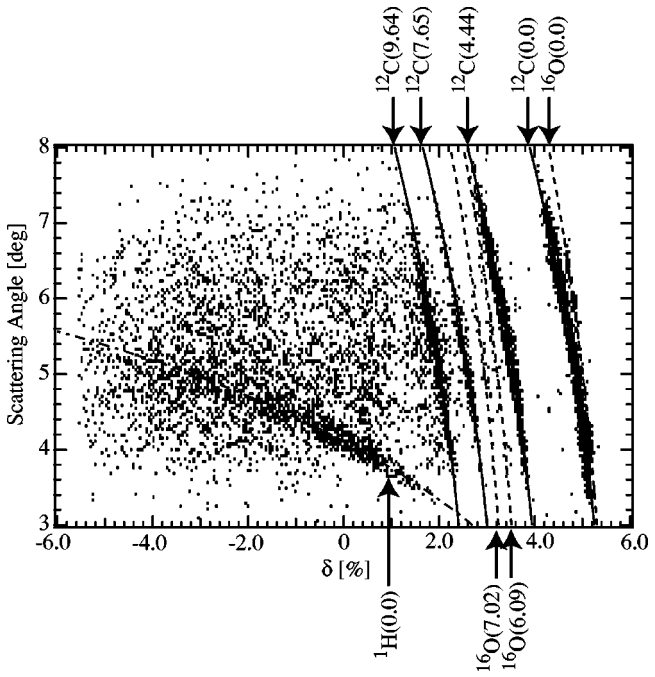

FIG. 2. Kinematic energy spectrum for elastic and inelastic scattering of the ^{9}Be beam off a carbon target with hydrogen and oxygen contamination. The horizontal axis is defined as the percentage energy deviation from the central ray. The solid, dashed, and dot-dashed lines are kinematics calculations for states in ^{12}C, ^{16}O, and ^{1}H, respectively. Aligning the known kinematics with the data provides a scattering angle calibration accurate to $\pm 0.05°$.

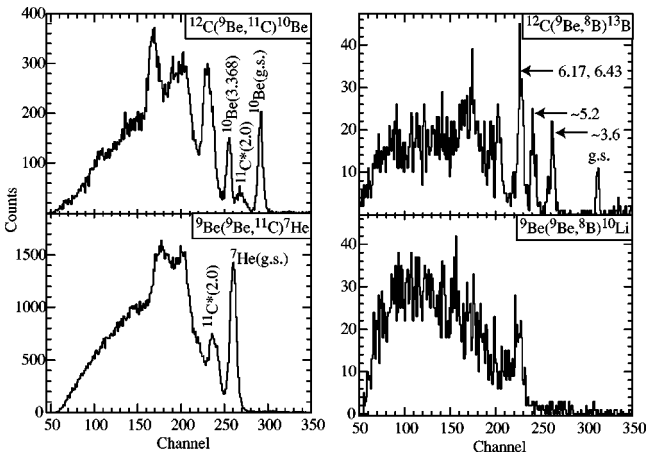

FIG. 3. ^{11}C (left) and ^{8}B (right) energy spectra for all reactions used in this experiment, at $\Theta_{lab}=3.5$-8.3 degrees, kinematically shifted to 0 degrees, and 40.1(1) MeV/nucleon. The states in ^{13}B labeled as $\sim$3.6 and $\sim$5.2 MeV correspond to groups of states that were populated at those energies. The ^{11}C states marked with an asterisk are doppler broadened by in-flight γ decay.

on the figure are kinematic calculations made at 40.1 MeV/nucleon. A small scattering angle offset of 0.25(5) degrees was added to all reconstructed scattering angles in order to align the spectrum with the calculations.

III. RESULTS AND DISCUSSION

Measured cross sections for all four reactions are listed in Table II. Uncertainties which are known (statistics and target thicknesses) are combined in quadrature and listed in the table. An unknown but estimated 10–50 % uncertainty on the integrated beam current is not included.

Figure 3 shows energy spectra of the ^{8}B and ^{11}C particles following the ^{12}C(^{9}Be,^{8}B)^{13}B, ^{9}Be(^{9}Be,^{8}B)^{10}Li, ^{12}C(^{9}Be,^{11}C)^{10}Be, and ^{9}Be(^{9}Be,^{11}C)^{7}He reactions at 40.1(1) MeV/nucleon. The spectrograph was positioned to accept reaction scattering angles between 3.5 and 8.3 degrees in the lab. The spectra were summed over all angles with the energy for each angle shifted to what it would be at 0°. The peaks in the ^{11}C energy spectra come from populating states in both the residual nuclei (^{10}Be and ^{7}He) and the ejectile. Only states in the residual nuclei appear in the ^{8}B spectrum because the excited states of ^{8}B are particle unbound and will break up before reaching the spectrograph focal plane detectors. Ten known states from the ground state up through 6.43 MeV in ^{13}B and the ground and first excited states in ^{10}Be were used for energy calibration. Contributions to the spectra from oxygen or other target contaminants can be ruled out due to the different kinematics.

TABLE II. Measured cross sections for four reactions used in this experiment at $E(^{9}\text{Be})=40.1$ MeV/nucleon.

Reaction	$\sigma_{lab}(\theta)(\mu$b/sr)
^{12}C(^{9}Be,^{8}B)^{13}B(g.s.)	0.42(7)
^{9}Be(^{9}Be,^{8}B)^{10}Li (lowest peak)	0.26(3)
^{12}C(^{9}Be,^{11}C)^{10}Be(g.s.)	12.3(12)
^{9}Be(^{9}Be,^{11}C)^{7}He(g.s.)	13.1(14)

The expected line shapes of the states in ^{10}Li have been calculated by Young *et al.* [14] and by Bertsch *et al.* [6]. The shapes of the *p*-wave states are well parameterized by a modified Breit-Wigner shape with an energy-dependent width, $\Gamma \sim E^{3/2}$ [26]. The calculations of [14] were fit with this parametrization and one from [6]; this parametrization was used as it fits the calculations slightly better. The parametrization of the *s*-wave state used here was a Breit-Wigner shape with an energy-dependent width, $\Gamma \sim E^{1/2}$, similar to that of Thoennessen *et al.* [17]. The angular momentum barrier of the *p*-wave states causes their width to increase more slowly with resonance energy than the *s*-wave states. For example, a 250 keV *p*-wave state is estimated to have a width around 100 keV, while an *s*-wave state at the same location would have a width well over 1 MeV.

The ^{10}Li spectrum (Fig. 3) was fit using a convolution of the estimated line shape with the experimental resolution. The experimental resolution was limited by kinematic broadening due to the finite primary beam emittance of $\sim 5\pi$ mm mrad in both transverse directions and target thickness effects. The ^{11}C energy resolution was dominated by target thickness, while the kinematic broadening due to the finite primary beam emittance dominated the ^{8}B energy resolution. The shape of the resolution function was dominantly Gaussian with a small Lorentzian component, deter-

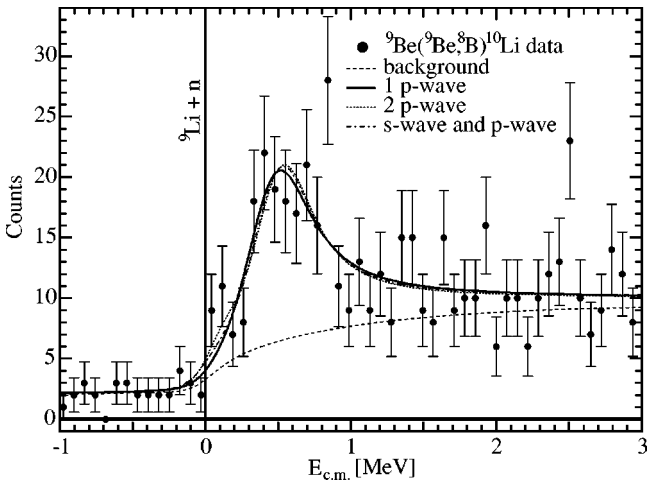

FIG. 4. ^{10}Li energy spectrum for the reaction ^{9}Be(^{9}Be,^{8}B)^{10}Li at $\Theta_{lab}=3.5$–8.3 degrees, kinematically shifted to 0 degrees. The solid line is the best fit to the data using a single *p*-wave resonance shape at $-S_n=500(60)$ keV with a width of 400(60) keV, including contributions from a constant plus a three-body background. The dashed and dot-dashed lines represent fits with two *p* waves and one *s* wave and one *p* wave, respectively. Both produce fits which are statistically less significant than the single *p*-wave resonance.

mined by applying the fitting procedure to the ^{7}He ground-state peak.

The function minimization routine AMOEBA was adopted from Press *et al.* [25], and used to fit the data using the maximum likelihood estimator. Figure 4 shows the calibrated energy spectra and the corresponding fits. The spectrum was fit from -1 to 3 MeV relative energy and the peak parameters are summarized in Table III. Contributions from a constant plus a three-body background (see Ref. [14]) were included in the fit and are shown in the figure.

An acceptable overall fit is achieved with a single *p*-wave state at $-S_n=500(60)$ keV and a width of $\Gamma=400(60)$ keV (see Fig. 3). Combinations of one *s* wave and one *p* wave, and two *p* waves provided fits which were statistically less significant due to the increased number of fit parameters. Inclusion of the extra s-wave or p-wave shape moved the 500 keV structure up 15 and 25 keV, respectively, and reduced its width by 50 keV in both cases. No other states in ^{10}Li were identified in this experiment, either because they were not populated, or the experimental resolution was insufficient. The 500 keV peak is probably the peak seen by Young *et al.* [14] and Bohlen *et al.* [15].

The errors were determined using a quadrature sum of several sources. Target thickness, beam energy, spectrometer angle, and ray-tracing techniques all play small roles (1–30 keV) and the uncertainties on the mass (1 keV) and excited states ($\leqslant 7$ keV) in ^{13}B and ^{10}Be are included. The differential target thicknesses were measured using the elastically scattered beam from the three targets. The absolute target thicknesses were determined by α-particle energy-loss measurement for two of the targets, and these measurements are consistent with the differential measurements. Statistical errors on the parameters dominate the uncertainties.

TABLE III. Different fits to the energy spectrum of ^{10}Li from the ^{9}Be(^{9}Be,^{8}B)^{10}Li reaction in the present work. The single *p*-wave fit provided the best fit to the data. See text for details.

States included in the fit	Peak location (keV)	Width (keV)
One *p* wave	500(60)	400(60)
Two *p* waves	100(60), 525(60)	50(50), 345(60)
One *s*-wave, one *p* wave	$\leqslant$50, 500(60)	$\leqslant$100, 400(60)

Because the 500 keV peak is relatively narrow, we conclude that it must be dominantly a *p*-wave state, based on previous calculations [6,14]. However, one reference suggests that the spin-parity assignment of the state cannot be extracted by line shape alone [26]. Clearly a measurement sensitive to the quantum numbers of the states involved should be performed.

IV. SUMMARY

This measurement represents another data point for the ^{10}Li puzzle and supercedes the earlier ^{9}Be(^{9}Be,^{8}B)^{10}Li reaction study by Wilcox *et al.* [12] because of the improved statistics and resolution. The quantum numbers of the states remain an open question, as do the exact shapes of the states. The energy spectrum is almost identical to that of Young *et al.* [14], except with $\approx$50% more statistics. This is quite remarkable considering that the experiments use different reactions with different net nucleon transfer. There is no evidence for a state at $\sim$250 keV in the present data. The excess of counts at threshold cannot be attributed to a state given the current experimental resolution and statistics, but the presence of a small enhancement is suggestive of one, as in the Young *et al.* [14] experiment. A different reaction or the same reaction made closer to zero degrees may populate the *s*-wave state more strongly. It would be desirable to repeat the Young *et al.* [14] experiment with better resolution and higher statistics, and the Bohlen *et al.* [15] experiment which populated the 240 keV state.

ACKNOWLEDGMENT

This work was supported by the National Science Foundation under Grant No. PHY-9528844.

[1] K. Riisager, Rev. Mod. Phys. **66**, 1105 (1994).
[2] J.S. Al-Khalili and J.A. Tostevin, Phys. Rev. Lett. **76**, 3903 (1996).
[3] P.G. Hansen, A.S. Jensen, and B. Jonson, Annu. Rev. Nucl. Part. Sci. **45**, 591 (1995).
[4] I. Thompson and M. Zhukov, Phys. Rev. C **49**, 1904 (1994).
[5] H. Esbensen, Phys. Rev. C **56**, 3054 (1997).
[6] G.F. Bertsch, K. Hencken, and H. Esbensen, Phys. Rev. C **57**,

1366 (1998).
[7] F.C. Barker and G.T. Hickey, J. Phys. G **3**, L23 (1977).
[8] B.A. Brown, Proceedings of the International Conference on Exotic Nuclei and Atomic Masses, Arles France, 1995, p. 451.
[9] N.A.F.M. Poppelier, A.A. Wolters, and P.W.M. Glaudemans, Z. Phys. A **346**, 11 (1993).
[10] J. Wurzer and H.M. Hofmann, Z. Phys. A **354**, 135 (1996).
[11] H.G. Bohlen *et al.*, Z. Phys. A **344**, 381 (1993).
[12] K.H. Wilcox, R.B. Weisenmiller, G.J. Wozniak, N.A. Jelley, D. Ashery, and J. Cerny, Phys. Lett. **59B**, 142 (1975).
[13] A.I. Amelin *et al.*, Yad. Fiz. **52**, 1231 (1990) [Sov. J. Nucl. Phys. **52**, 782 (1990)].
[14] B.M. Young, W. Benenson, J.H. Kelley, N.A. Orr, R. Pfaff, B.M. Sherrill, M. Steiner, M. Thoennessen, J.S. Winfield, J.A. Winger, S.J. Yennello, and A. Zeller, Phys. Rev. C **49**, 279 (1994).
[15] H.G. Bohlen, W. von Oertzen, Th. Stolla, R. Kalpakchieva, B. Gebauer, M. Wilpert, Th. Wilpert, A.N. Ostrowski, S.M. Grimes, and T.N. Massey, Nucl. Phys. **A616**, 254c (1997).
[16] R.A. Kryger *et al.*, Phys. Rev. C **47**, R2439 (1993).
[17] M. Thoennessen *et al.*, Phys. Rev. C **59**, 111 (1999).
[18] M. Zinser *et al.*, Nucl. Phys. **A619**, 151 (1997).
[19] J.A. Nolen, Jr., A.F. Zeller, B. Sherrill, J.C. DeKamp, and J. Yurkon, MSU-NSCL Report No. MSU-694 (1989).
[20] B.M. Sherrill, D.J. Morrissey, J.A. Nolen, Jr., N. Orr, and J.A. Winger, Nucl. Instrum. Methods Phys. Res. B **70**, 298 (1992).
[21] J. Yurkon, D. Bazin, W. Benenson, D.J. Morrissey, B.M. Sherrill, D. Swan, and R. Swanson, Nucl. Instrum. Methods Phys. Res. A **422**, 291 (1999).
[22] M. Berz, Nucl. Instrum. Methods Phys. Res. A **298**, 473 (1992).
[23] M. Berz, K. Joh, J.A. Nolen, B.M. Sherrill, and A.F. Zeller, Phys. Rev. C **47**, 537 (1993).
[24] G. Audi and A.H. Wapstra, Nucl. Phys. **A565**, 1 (1993).
[25] W.H. Press, S.A. Teukolsky, W.T. Vetterling, and B.P. Flannery, *Numerical Recipes in C* (Cambridge University Press, Cambridge, 1992), p. 408.
[26] K.W. McVoy and P. Von Isacker, Nucl. Phys. **A576**, 157 (1994).